Antenna and Multipath Calibration System for High Accuracy Geophysical Applications of GPS

Kwan-Dong Park[1] (kdpark@cfa.harvard.edu), Pedro Elósegui[1], James L. Davis[1], Brian E. Corey[2], and Arthur E. Niell[2]

([1]Harvard-Smithsonian Center for Astrophysics, Cambridge, MA.; [2]MIT Haystack Observatory, Westford, MA.)

1. Introduction

Geophysical applications of the Global Positioning System (GPS) for studies such as global sea level change and glacial isostatic adjustment require a very high accuracy (1 mm/year) in determining the site velocity, especially its vertical component. However, site-specific errors such as signal scattering and multipath remain problematic. For the purpose of characterizing site-specific GPS phase measurement errors, we have developed an Antenna and Multipath Calibration System (AMCS). The AMCS consists of a high-gain, multipath-free, 3-m diameter parabolic antenna and two Trimble GPS receivers. We present a synopsis of the system, zero-motion AMCS test results, and discussion of error sources.

2. Elements of the AMCS

The AMCS consists of a:

- High-gain, "multipath-free" parabolic reflector radio antenna with high directionality
- Two identical geodetic GPS receivers
- Short-baseline to GPS antenna to be calibrated for multipath, scattering, and phase-center variations

3. Zero-motion AMCS Tests

In this type of tests, the parabolic antenna is pointed at a constant position in the sky and satellites were allowed to drift in and out of the antenna beam. In the beginning to a test, two receivers connect to the standard geodetic antenna (to be calibrated) and collects data in the ZBL (**Z**ero-**B**ase**L**ine) mode. Then, one receiver switches to the parabolic antenna and collects the data in the AMCS-mode.

The model for the ZBL-mode phase $\Delta\phi^k$ for the kth satellite is:

$$\Delta\phi^k(t) = \dot{\rho}(t)\Delta T + \Delta\phi_o^k \qquad (1)$$

where $\Delta\phi^k(t)$ is in meters, ΔT is the clock offset, assumed constant over the entire analysis, $\dot{\rho}(t)$ is the range-rate between the antenna and the satellite, and $\Delta\phi_o^k$ is a constant offset in meters, one per satellite. We used the broadcast ephemerides to calculate the range-rates.

The model for the AMCS-mode phase $\Delta\varphi^K$ is:

$$\Delta\varphi^K(t) = \dot{\rho}(t)\Delta\hat{T} + \Delta\hat{\phi}_{1,o}^K + \lambda N + \hat{s}\cdot\vec{b} + C\cos\epsilon \qquad (2)$$

The range-rate is $\dot{\rho}(t)$ as before, and $\Delta\hat{T}$ is the receiver clock offset estimated from the ZBL-mode analysis. Similarly, $\Delta\hat{\phi}_{1,o}^K$ is the phase offset for the first ZBL-mode group, estimated in the ZBL-mode analysis. N is the integer cycle offset. The satellite topocentric unit vector is $\hat{s}$, and $\vec{b}$ is the AMCS baseline vector. The final term in Equation 2 accounts for the elevation-axis offset. C is a constant determined by surveys and ϵ is the satellite elevation angle. No "feed rotation" corrections were applied.

4. Results and Discussion

We present an analysis of zero-motion AMCS tests conducted in May, 2000 (refer to Table 1). The parabolic antenna was pointed at a constant position in the sky (aiming at the direction of PRN 2) and satellites were allowed to drift in and out of the beam.

Table 1. Test data sets. θ and ϵ is the azimuth and elevation angles for the direction of the parabolic antenna. Data span is in seconds.

Data Set	Day	PRN	θ (deg)	ϵ (deg)	Data Span ZBL	Data Span AMCS
Case 1	May 1	2	255.4	79.8	590	670
Case 2	May 1	2	191.7	70.9	580	680
Case 3	May 2	2	255.4	79.8	590	480
Case 4	May 2	2	191.7	70.9	580	710

For each set, ZBL data was processed first and the receiver clock offset and the phase offset of each satellite were determined in the least-squares estimation. In the next step, estimated values from the ZBL-mode analysis were used in the AMCS-mode analysis without any interpolation. In Equation 2, no parameter was estimated. $\Delta\hat{T}$ and $\Delta\hat{\phi}_{1,o}^K$ in Equation 2 are from the ZBL-mode estimation. The fourth and last terms are computed using satellite azimuth and elevation angles and field measurements of the geometry between the two antennas. λN_r was determined such that $\Delta\varphi^K(t) - \dot{\rho}(t)\Delta\hat{T} - \Delta\hat{\phi}_{1,o}^K - \hat{s}\cdot\vec{b} - D\cos\epsilon$ have a zero mean. Thus, N is not fixed as an integer value. The reason is because we liked to make the AMCS-mode residuals to have a near-zero mean. It can be fixed as an integer number later.

Table 2. Comparison of receiver clock offset, ZBL-mode RMS, and AMCS-mode RMS.

Data Set	ZBL ΔT (msec)	ZBL RMS (mm)	AMCS RMS (mm)
Case 1	0.33 ± 0.5	0.56	1.74
Case 2	0.35 ± 0.4	0.54	1.44
Case 3	0.34 ± 0.4	0.46	1.86
Case 4	0.37 ± 0.6	0.58	1.92

American Geophysical Union, Spring Meeting, 2001. **T52A-14**

The estimated values of the receiver clock offset are in the range between 0.33 and 0.37 msec (see Table 2). The root-mean square (RMS) of the ZBL-mode data is below 0.6 mm in all 4 cases. The AMCS-mode RMS is about three times higher than that of the ZBL-mode, but is consistently below 2.0 mm.

An example plot of the L_1 phase residuals is shown below. This plot shows ZBL-mode residuals (of 5 satellites) on the left-hand side and AMCS-mode residuals (of PRN 2 and denoted by red $\times$) on the right-hand side. Systematic trends are visible in the ZBL-mode residuals. Some of the variations appear to be satellite independent and so are not variations of ΔT. Some of the variations are satellite dependent, or at least the scatter seems satellite dependent. There's also a hint that the variations are similar from one day to the next. The AMCS-residuals show highly systematic variations. The possible reasons include parabolic antenna pointing offset errors, survey errors in measuring the relative geometry of the two antennas, parabolic antenna beam pattern errors and low SNR (Signal-to-Noise Ratio) in the AMCS-mode data collection. A series of tests are underway to pinpoint the error sources.

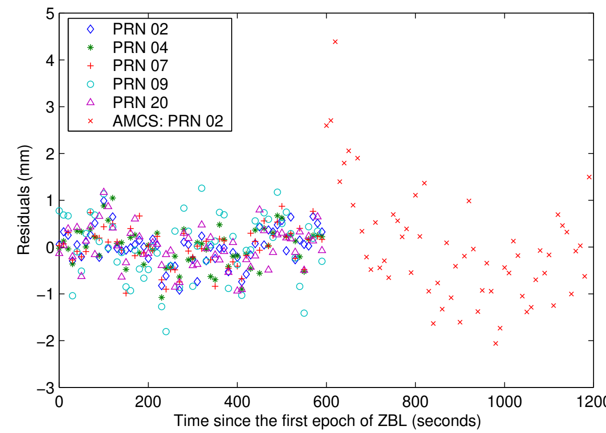

5. Future Work

- Tests at Haystack Observatory:
  - Test antenna mechanical and electrical stability
  - Improve algorithms for multipath data analysis
- Transfer the system to the UNAVCO facility
- Work with UNAVCO and IGS to prioritize and coordinate site visits and develop a standardized site implementation scheme

6. Acknowledgements

This work is supported by NSF grant EAR-9708251. We acknowledge the extensive technical and equipment support from the UNAVCO-Boulder facility.